Supporting Information for

Multi-Functional PEDOT-Engineered Sodium Titanate Nanowires for Sodium-Ion Batteries with Synchronous Improvements in Rate Capability and Structural Stability

Qing Zhang,[a] Yi He,[a] Peng Mei,[a] Xun Cui,[a,b] Yingkui Yang,*[a] and Zhiqun Lin*[b]

[a] *Hubei Engineering Technology Research Centre of Energy Polymer Materials, School of Chemistry and Materials Science, South-Central University for Nationalities, Wuhan 430074, China*

E-mail: ykyang@mail.scuec.edu.cn

[b] *School of Materials Science and Engineering, Georgia Institute of Technology, Atlanta, GA 30332, USA*

E-mail: zhiqun.lin@mse.gatech.edu

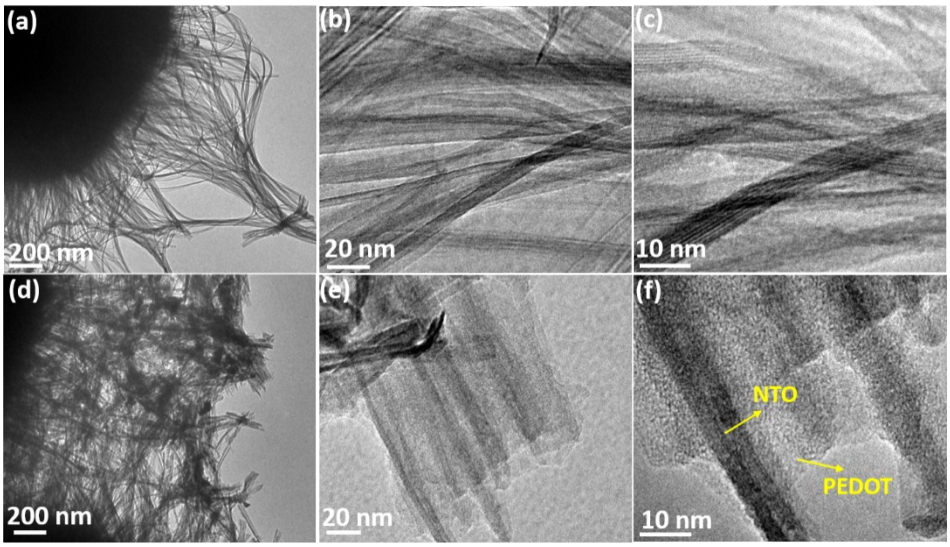

Fig. S1 TEM images of (a-c) NTO, and (d-f) PEDOT@NTO with different magnifications.

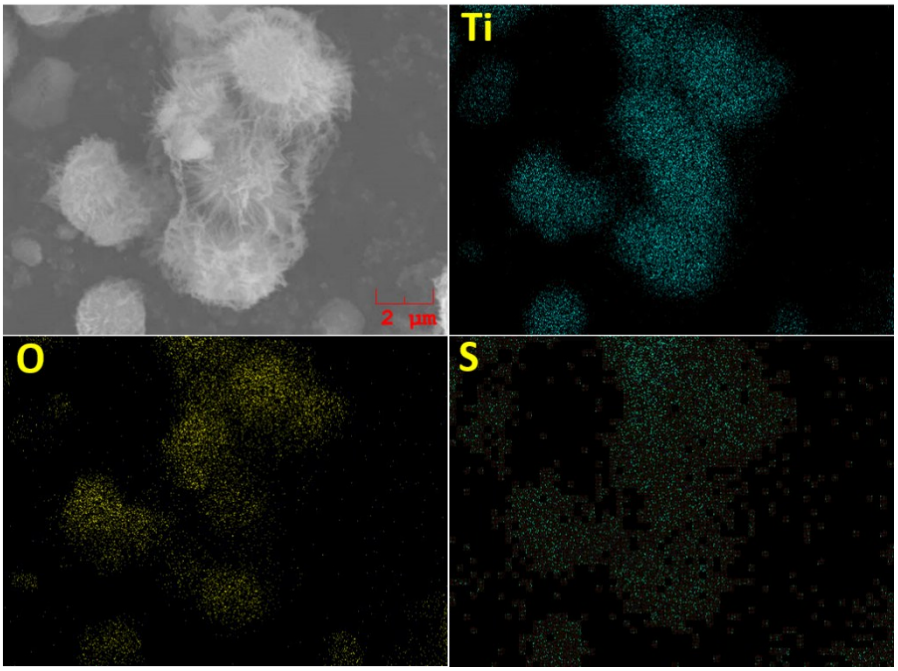

Fig. S2 A SEM image and elemental mapping patterns (Ti, O, S) of PEDOT@NTO.

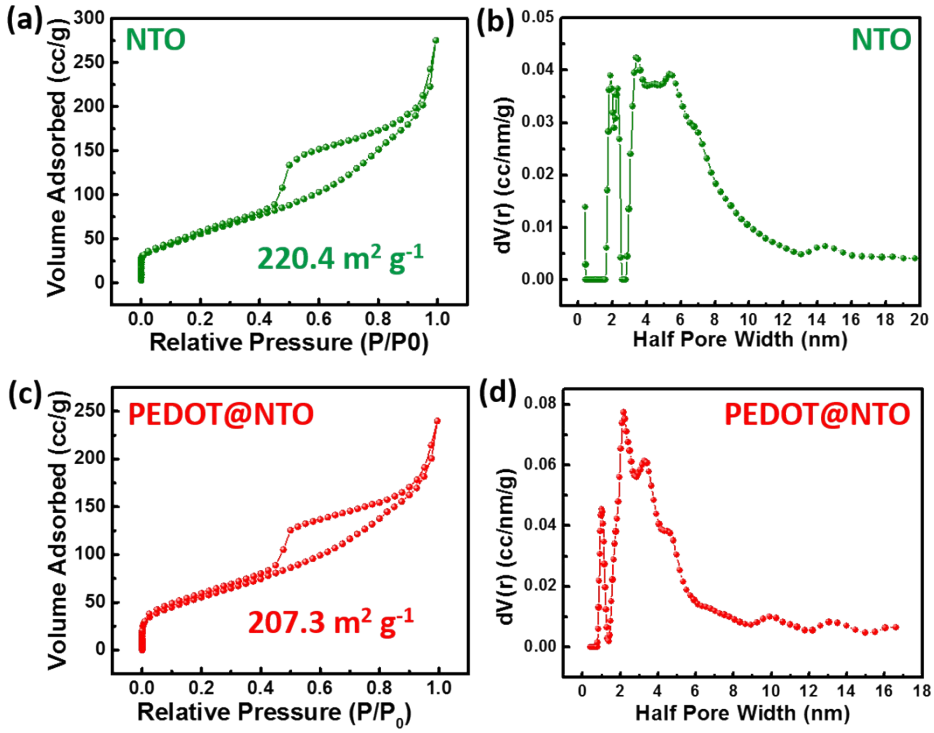

Fig. S3 Nitrogen adsorption/desorption isotherms and pore size distributions of (a, b) NTO and (c, d) PEDOT@NTO.

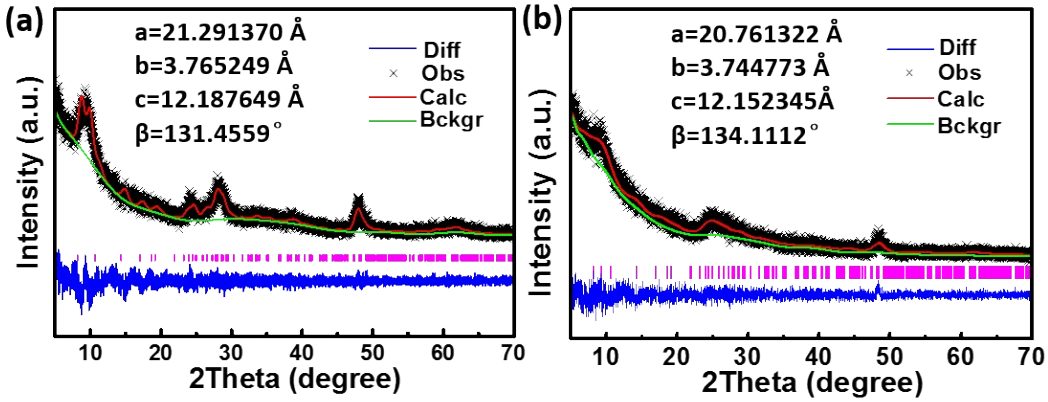

Fig. S4 The Rietveld refinement of (a) the as-prepared NTO and (b) PEDOT@NTO.

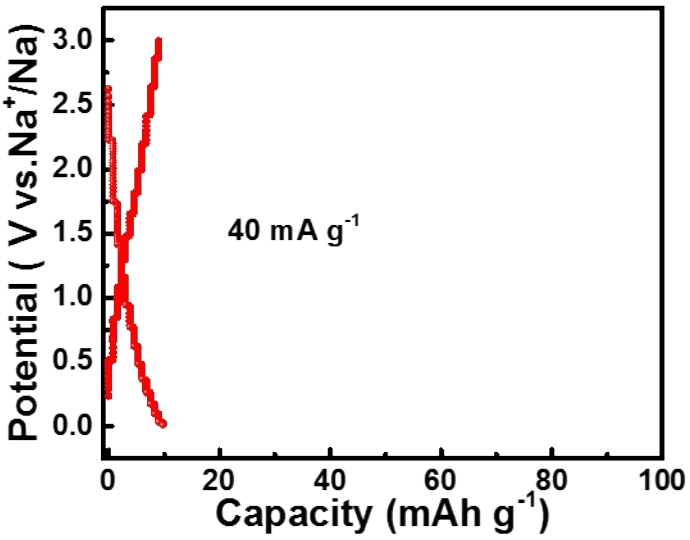

Fig. S5 Typical discharge/charge curves of pure PEDOT at 40 mA g^{-1}.

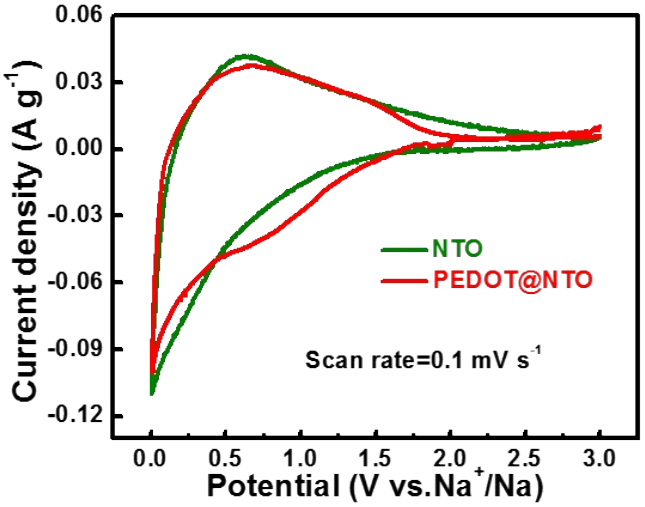

Fig. S6 CV curves of PEDOT@NTO and NTO at 0.1 mV s^{-1}.

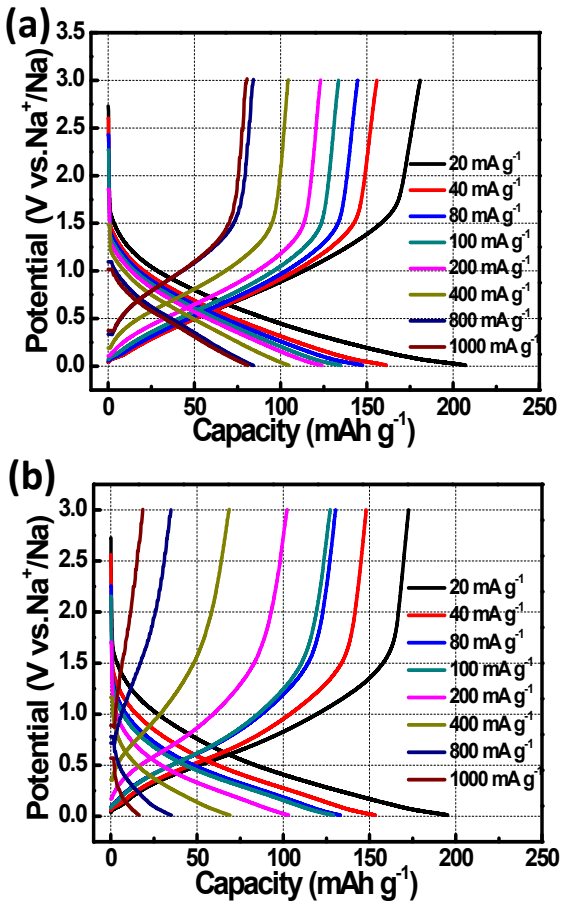

Fig. S7 Discharge-charge curves of (a) NTO and (b) PEDOT@NTO at different current densities.

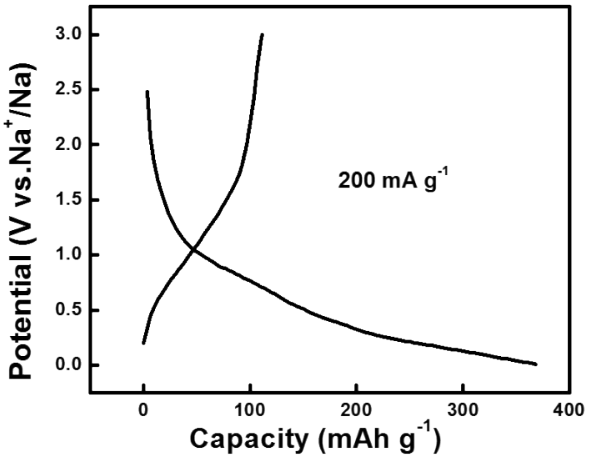

Fig. S8 The first discharge/charge curves of PEDOT@NTO at 200 mA g^{-1}.

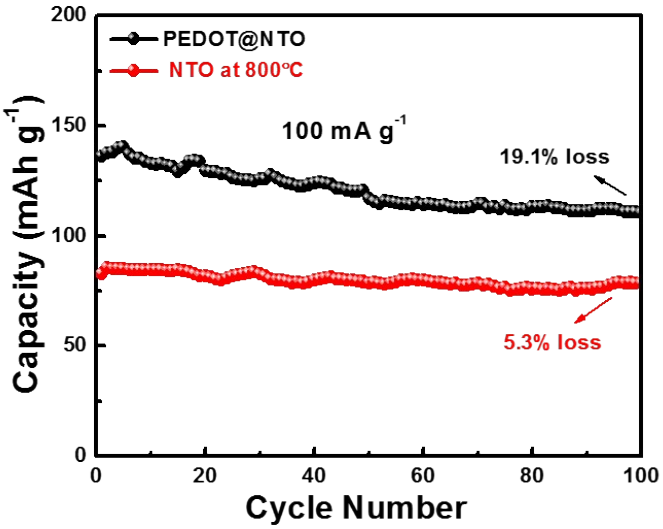

Fig. S9 Cycling performance of the as-produced PEDOT@NTO and NTO treated at 800°C at a current density of 100 mA g^{-1}.

The previous reports have suggested that the capacity drop in the initial 100 cycles is mainly ascribed to the side reactions and stabilization of SEI films for sodium titanate anodes because of relatively large specific areas and the existence of water molecules (*ACS Appl. Mater. Interfaces* 2017, 9: 11669-11677; *Electrochim. Acta* 2016, 211: 430-436; *Adv. Funct. Mater.* 2016, 26: 3703-3710). In order to approve the suppositions, the as-prepared NTO nanowires were further annealed at 800°C to remove water molecules and reduce specific surface area. **Figure S9** shows the cycling performance of the annealed NTO and PEDOT@NTO. It can be found that the capacity drop of the dehydrated NTO in the initial 100 cycles is only 5.3%, which is much less than that of PEDOT@NTO (19.1%). This finding identifies that the capacity loss in the initial few cycles is mainly ascribed to the side reactions for NTO nanomaterials.

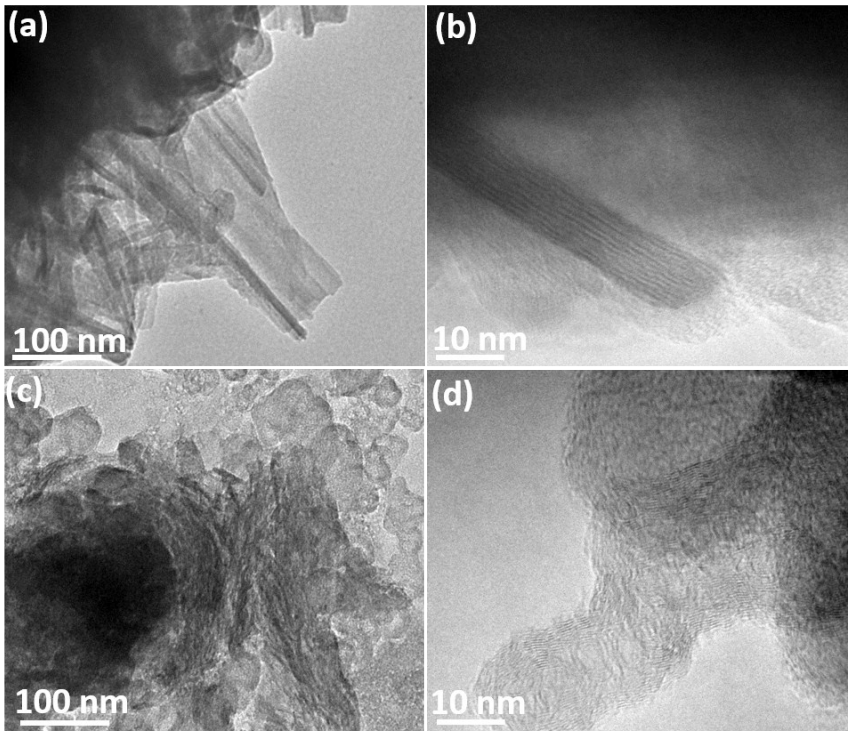

Fig. S10 TEM images of (a, b) PEDOT@NTO and (c, d) NTO after cycling.

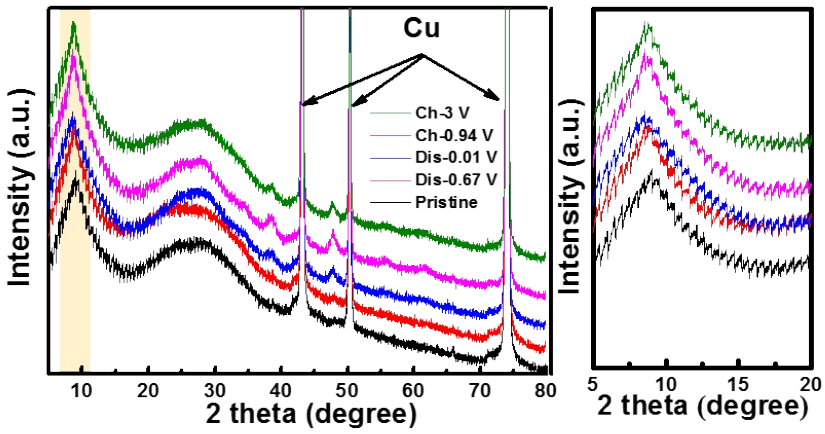

Fig. S11 The *ex-situ* XRD patterns collected during the first discharge/charge.

Table S1. A survey of sodium storage performance of NTO and their composites

Electrode description	Capacity	Rate capability	Cycling stability	Ref.
PEDOT@NTO nanowires	**200.1 mAh g^{-1} at 20 mA g^{-1}**	**80.5 mAh g^{-1} at 1,000 mA g^{-1}**	**76.4% after 1,000 cycles at 200 mA g^{-1}**	**This work**
3D $Na_2Ti_3O_7$ microflowers	173 mAh g^{-1} at 50 mA g^{-1}	73.8 mAh g^{-1} at 800 mA g^{-1}	85% after 1100 cycles at 400 mA g^{-1}	[1]
3D flower-like $NaHTi_3O_7$ nanotubes	242.8 mAh g^{-1} at 20 mA g^{-1}	80 mAh g^{-1} at 100 mA g^{-1}	36.8% (76.3 mAh g^{-1}) after 100 cycles at 100 mA g^{-1}	[2]
$Na_2Ti_3O_7$ nanowires@ carbon cloth	184.5 mAh g^{-1} at 35.4 mA g^{-1}	54.9 mAh g^{-1} at 885 mA g^{-1}	96% after 200 cycles at 354 mA g^{-1}	[3]
$Na_2Ti_3O_7$/C composite	133.4 mAh g^{-1} at 89 mA g^{-1}	79.5 mAh g^{-1} at 890 mA g^{-1}	76.4% after 100 cycles at 890 mA g^{-1}	[4]
$Na_2Ti_6O_{13}$ nanorods	76.1 mAh g^{-1} at 50 mA g^{-1}	37.2 mAh g^{-1} at 300 mA g^{-1}	85.3 % after 50 cycles at 50 mA g^{-1}	[5]
$Na_2Ti_3O_7$/C composite	215 mAh g^{-1} at 20 mA g^{-1}	80 mAh g^{-1} at 500 mA g^{-1}	40.5% after 50 cycles at 200 mA g^{-1}	[6]
Flower-like $Na_2Ti_2O_4(OH)_2$	154 mAh g^{-1} at 20 mA g^{-1}	75 mAh g^{-1} at 1000 mA g^{-1}	76% after 200 cycles at 100 mA g^{-1}	[7]
Sodium titanate nanotube array	222 mAh g^{-1} at 50 mA g^{-1}	66 mAh g^{-1} at 800 mA g^{-1}	73% after 200 cycles at 400 mA g^{-1}	[8]

References

(1) Anwer, S.; Huang, Y.; Liu, J.; Liu, J.; Xu, M.; Wang, Z.; Chen, R.; Zhang, J.; Wu, F., Nature-inspired $Na_2Ti_3O_7$ nanosheets-formed three-dimensional microflowers architecture as a high-performance anode material for rechargeable sodium-ion batteries. *ACS Appl. Mater. Interfaces* **2017**, *9*, 11669-11677.

(2) Wang, S.; Wang, W.; Zhan, P.; Yuan, Y.; Jiao, K.; Jiao, H.; Jiao, S., 3D flower-like $NaHTi_3O_7$ nanotubes as high-performance anodes for sodium-ion batteries. *J. Mater. Chem. A* **2015**, *3*, 16528-16534.

(3) Li, Z.; Shen, W.; Wang, C.; Xu, Q.; Liu, H.; Wang, Y.; Xia, Y., Ultra-long $Na_2Ti_3O_7$ nanowires@carbon cloth as a binder-free flexible electrode with a large capacity and long lifetime for sodium-ion batteries. *J. Mater. Chem. A* **2016**, *4*, 17111-17120.

(4) Yan, Z.; Liu, L.; Shu, H.; Yang, X.; Wang, H.; Tan, J.; Zhou, Q.; Huang, Z.; Wang, X., A tightly integrated sodium titanate-carbon composite as an anode material for rechargeable sodium ion batteries. *J. Power Sources* **2015**, *274*, 8-14.

(5) Li, P.; Wang, P.; Qian, S.; Yu, H.; Lin, X.; Shui, M.; Zheng, X.; Long, N.; Shu, J., Synthesis of $Na_2Ti_6O_{13}$ nanorods as possible anode materials for rechargeable lithium ion batteries. *Electrochim. Acta* **2016**, *187*, 46-54.

(6) Ding, C.; Nohira, T.; Hagiwara, R., Electrochemical performance of $Na_2Ti_3O_7$/C negative electrode in ionic liquid electrolyte for sodium secondary batteries. *J. Power Sources* **2017**, *354*, 10-15.

(7) Babu, B.; Shaijumon, M. M., High performance sodium-ion hybrid capacitor based on $Na_2Ti_2O_4(OH)_2$ nanostructures. *J. Power Sources* **2017**, *353*, 85-94.

(8) Wang, X.; Li, Y.; Gao, Y.; Wang, Z.; Chen, L., Additive-free sodium titanate nanotube array as advanced electrode for sodium ion batteries. *Nano Energy* **2015**, *13*, 687-692.